[Frontiers in Bioscience, Landmark, 21, 1211-1221, June 1, 2016]

Photo-thermal therapy of bladder cancer with Anti-EGFR antibody conjugated gold nanoparticles

Chieh Hsiao Chen[1,2], Yi-Jhen Wu[1], Jia-Jin Chen[1]

[1]Institute of BioMedical Engineering, National Cheng Kung University, Tainan, Taiwan, [2]Department of Urology, China Medical University Beigang Hospital, Yunlin, Taiwan

TABLE OF CONTENTS

1. ABSTRACT

The aim of this study was to enhance the effectiveness of photo thermal therapy (PTT) in the targeting of superficial bladder cancers using a green light laser in conjunction with gold nanoparticles (GNPs) conjugated to antibody fragments (anti-EGFR). GNPs conjugated with anti-EGFR-antibody fragments were used as probes in the targeting of tumor cells and then exposed to a green laser (532nm), resulting in the production of sufficient thermal energy to kill urothelial carcinomas both *in vitro* and *in vivo*. Nanoparticles conjugated with antibody fragments are capable of damaging cancer cells even at relatively very low energy levels, while non-conjugated nanoparticles would require an energy level of 3 times under the same conditions. The lower energy required by the nanoparticles allows this method to destroy cancerous cells while preserving normal cells when applied *in vivo*. Nanoparticles conjugated with antibody fragments (anti-EGFR) require less than half the energy of non-conjugated nanoparticles to kill cancer cells. In an orthotopic bladder cancer model, the group treated using PTT presented significant differences in tumor development.

2. INTRODUCTION

The bladder is a hollow and distensible organ used to store urine. It is composed of mucosa, submucosa, detrusor muscle, and perivesical fat. Bladder cancer is the second most common genitourinary malignant disease in the US and Southeast Asia. One prevalent type of bladder cancer, referred to as urothelial carcinoma (UC), originates in the mucosa layer. UC accounts for more than 90% of bladder cancers. The remaining 10% include squamous cell carcinoma (SCC, 7-8%), adenocarcinoma (1-2%), and carcinosarcoma (<1%) (1). The superficial (non-muscle invasive) form of the disease accounts for the majority (70-85%) of all diagnosed cases (2-4). To curb disease progression and improve patient quality of life, developing methods to treat superficial bladder cancer (stage Tis, Ta and T1) directly is essential.

Intravesical installation of Bacillus Calmettte-Guerin (BCG) or chemotherapy agents such as Mitomycin C, Adriamycin, Epirubicin or Thiotepa are commonly used as adjuvant therapies following transurethral resection of bladder tumors (TURBT) (5, 6). Specifically, the chemical agent Mitomycin C inhibits the synthesis of DNA, RNA, and proteins, thereby suppressing the proliferation of cancer cells. Nevertheless, side effects such as chemical cystitis (in 67%), haematuria (23%), fever (25%), and frequent urination (71%) can be quite serious (1). BCG is the most common form of intravesical therapy for superficial bladder cancer; however, many studies have reported that this agent is only able to delay early recurrence (7). Indeed, BCG and chemotherapy are prone to high recurrence rates (40%-50%) and rapid disease progression, and methods that are able to target superficial bladder cancer (stage Tis, Ta, T1) directly have not yet been developed.

Nanotechnology is widely used in the detection and treatment of breast cancer (8, 9), oral cavity cancer (10, 11), lung carcinomas (12), cervical cancer, and brain cancer (13). Compared with other types of nanoparticles, such as core-shell silica nanoparticles, cerium oxide (CeO2) (14), TiO2 (15), ZnO (16), magnetic nanoparticles (17) and quantum dots (18), Gold nanoparticles (GNPs) are non-cytotoxic (19) and have excellent chemical stability as well as a high affinity to biomolecules used in the treatment and detection of cancer (20, 21). GNPs can be used as a replacement for traditional adjuvant therapy in the treatment of superficial bladder cancer. This study hypothesized that photothermal therapy (PTT) using GNPs would help reduce side effects and disease recurrence. Our findings reveal that the laser energy required to damage GNP-treated cancer cells is far below that of cells that were not treated with GNPs (22). The markers of urothelial carcinoma include Epidermal Growth Factor Receptor (EGFR) (23), mucin7 (MUC7) (24), and cytokeratin 20 (CK20) (25). The antibody on the GNPs can target the overexpressed antigen in the tumor, which can enhance the effectiveness of cancer treatment. Furthermore, this approach requires a shorter treatment time to achieve obvious effects and can also induce a state of hyperthermia with relatively low laser power, thereby preventing injury to nearby normal tissue (22).

3. MATERIALS AND METHODS

3.1. Synthesis of gold nanoparticles

GNPs were synthesized at an average size of 47 nm through chemical reduction in accordance with the method proposed by Kimling *et al* (26). Specifically, gold chloride trihydrate (Sigma) was diluted in D.D. water (Millipore) to a final concentration of 1.0×10^{-3} M. We then added 34.6×10^{-3} M trisodium citrate (J.T. Baker) to the boiling chloroauric acid solution under vigorous stirring until the citrate was thoroughly dispersed. The electropositive surface of the GNPs absorbed anions in the solution to attain a stable state of suspension. When the color turned purplish red, the GNP solution was removed from the heat and held at room temperature to cool for 30 min. The particle suspension was then centrifuged and diluted in 20×10^{-3} M HEPES buffer (pH 7.4, Sigma) to a final concentration possessing an optical density of 0.8 at 532 nm, which indicated the concentration of 0.24 nM according to the Beer-Lambert Law. To ensure sterility, the particle suspension was filtered using a Millipore filter of 0.22 μM.

3.2. Field emission scanning electron microscopy (FE-SEM)

To confirm the presence of GNPs on the surface of the cancer cells, we prepared biological specimens for FE-SEM (UltraPlus) as follows. First, we added 1 ml of GNPs solution with anti-EGFR fragments to 6-well culture plates with an equal volume of fresh RPMI 1640 medium. Following incubation for 30 min, the samples were washed three times with PBS and fixed in 4% paraformaldehyde for 20 min. The cells were then dehydrated for 5 min using ethyl alcohol in a sequence ratio of 45%, 60%, 75%, 90%, 95%, and 99.9%. To enhance electrical conductivity, the specimens were fixed on a copper strip using carbon tape and coated with carbon prior to observation.

3.3. Sample preparation for transmission electron microscopy (TEM)

TEM (Jeol JEM-1400) was used to confirm the distribution of GNPs in the specimen. Trypsin-EDTA was used to separate $4x10^5$ cells from the culture plate for placement in a 1.5 ml Eppendorf tube. The TCC cells were then incubated using 1 ml of GNPs solution with anti-EGFR fragments. After 30 min, the cells were washed in phosphate buffer solution three times and subjected to centrifugation before being fixed in 4% paraformaldehyde for 30 min. To enhance preservation, the cells were post-fixed in 1.3% aqueous osmium tetroxide (OsO4) at 4 ºC for 2 h.

The samples were washed three more times and then dehydrated with a graded series of ethyl alcohol at 50%, 70%, 85%, 95% (10 min), and 99.9% (2 times, 20 min each). The samples were then infiltrated with a mixture of alcohol and epoxy resin (at a 1:1 ratio) at 4 ºC for 6 h, followed by infiltration with pure resin overnight (16 h at 4 ºC and 6 h at room temperature), during which the resin was changed twice. The cells were then embedded in epoxy resin by inverting BEEM capsules and heating them to approximately 70 ºC in an oven for one day to promote polymerization (hardening) in the resin. Finally, the hardened resin was prepared as thin sections (approximately 70 nm) using an ultra-microtome, and lead citrate staining was employed to reveal the structure of the cell membrane.

© 1996-2016

3.4. Preparation of antibody fragments for labeling of gold nanoparticles

Enhancing the conjugation and decreasing the molecular weight of immunized gold nanoparticles is an effective way to (1) increase their stability and specificity and (2) prevent precipitation. Therefore, this study generated antibody fragments to enhance the efficiency of conjugation with GNPs (27). As GNPs have a strong affinity to sulfhydryl groups, we adopted a reduction method for the process of conjugation.

Antibodies were reduced by cleaving the disulphide bonds bridging the heavy chains with 2-mercaptoethylamine, while leaving the disulfides between the light and heavy chains intact. Thus, each antibody fragment had one heavy chain, one light chain, and one antigen binding site (27).

The reduction of antibody fragments was achieved using the method outlined by Yoshitake *et al.* (28). Specifically, antibodies were dissolved at a concentration of 10 mg/ml in 20 mM sodium phosphate buffer (PH 7.2) containing 150 mM NaCl and 10 mM ethylene diamine tetraacetic acid (EDTA). We then added 6 mg of 2-mercaptoethylamine (2-MEA) to the antibody solution and incubated the reaction mixture at 37 ºC for 90 min. Finally, the reduced antibodies were purified using a gel filtration column equilibrated with the same buffer containing 5 mM EDTA for the removal of excess 2-MEA. The dialysis buffer was changed twice in order to ensure that the desalted antibodies had been purified. The antibody fragments were than combined with the GNP suspension and incubated at 37 ºC for 30 min in a humidified tissue culture incubator. Finally, bovine serum albumin was added to block the exposed GNPs.

3.5. Culturing of bladder tumor cells

Malignant urothelial cell lines MBT-2 (mrine) and 9202 (human) were obtained from Tri-Service General Hospital, Taipei, Taiwan. All cell lines were grown at 37 ºC and maintained in a humidified atmospheric pressure chamber under 5% CO_2. Cells were cultured in Roswell Park Memorial Institute 1640 (GIBCO-BRL) medium supplemented with 10% Fetal Bovine Serum (FBS) and 1% penicillin- streptomycin. The medium was changed three times per week.

3.6. Flow cytometry system

We used flow cytometry (BD FACSCanto) to obtain an accurate quantification of cell lines. For this, 2×10^7 cells/ml were washed with PBS containing 0.03% sodium azide before 50µl of the cell suspension (approximately 1×10^6 cells) was loaded into a test tube. Cells were then incubated with diluted anti-EGFR antibodies (0.005 mg/ml) at 4º C in a darkened room for 30 min before being centrifuged with 3 ml PBS at 1500 rpm (300 xg) for 5 min to remove unbound antibody fragments. Cells were subsequently stained with 0.5 ml of fluorescein (APC) secondary antibodies (1:1000) at 4º C for 30 min in a darkened room. Finally, the stained cells were subjected to repeated centrifugation for 5 min with PBS to remove excess secondary antibody material. The remaining cells were preserved in 0.5 ml cold PBS with 1% paraformaldehyde prior to analysis (which was conducted within 24 h).

3.7. *In vitro* laser therapy

Cells were cultured in a 6-well tissue culture plate at a seeding density of 200,000 cells/well for 4 days. At the end of the incubation period, GNPs conjugated with antibody fragments were added to culture plates at a concentration of 1 ml per well (GNPs: RPMI = 1:1). Following incubation at 37º C for 30 min, the anti-EGFR/GNP fragments were washed three times with medium to remove unbound immunized nanoparticles. A 532 nm green light laser system (IDAS) was used to provide stable, safe power for the experiments. This wavelength was selected because it overlaps the absorption region of the GNPs, thereby promoting thermal efficiency. Pulse mode was employed to prevent the medium from overheating. Following incubation for 30 min, cells immersed in GNP suspension were exposed to laser light (532 nm) at various power densities for 500 shots. To evaluate cell viability, images of cells stained with 0.4% trypan blue (Sigma) were obtained using a Motic AE21 microscope at a magnification of 40X. The temperature of the treatment area was determined using an IR thermometer.

3.8. Orthotopic bladder cancer animal model

An animal tumor study was performed to verify the efficacy of this therapy. For this, we adopted the common orthotopic bladder cancer model developed by Xiao *et al.* (29). Credé's method was employed to evacuate accumulated urine from anaesthetized C3H mice using Avertin 1.2% (0.0.14-0.0.18 ml/g). The mouse bladders were catheterized using a 24-gauge plastic cannula with lubricant for the instillation procedures. To facilitate the seeding of tumor cells, the bladder mucosa (glycosaminoglycan layer) was destroyed using 0.4ml of 0.1N hydrochloric acid (HCl) and neutralized with 0.4ml sodium hydroxide (NaOH) of 0.1N. After waiting for 15 s, the mouse bladders were flushed using sterile phosphate-buffered saline (PBS). PBS was immediately drained from the bladder via instillation. A total of 1×10^6 MBT2 tumor cells were then injected into the bladder lumen via the urethra. We evaluated tumor progression by sacrificing the mice for pathological examination at 2 weeks post-inoculation. The implantation rate was 83.3% (25/30).

3.9. Laser therapy: *in vivo* mouse model

To confirm the efficacy of photothermal therapy in superficial bladder cancer, the mice underwent treatment 3 days after the implantation of cancer cells. The anesthesia was done and inserted the urethral

© 1996-2016

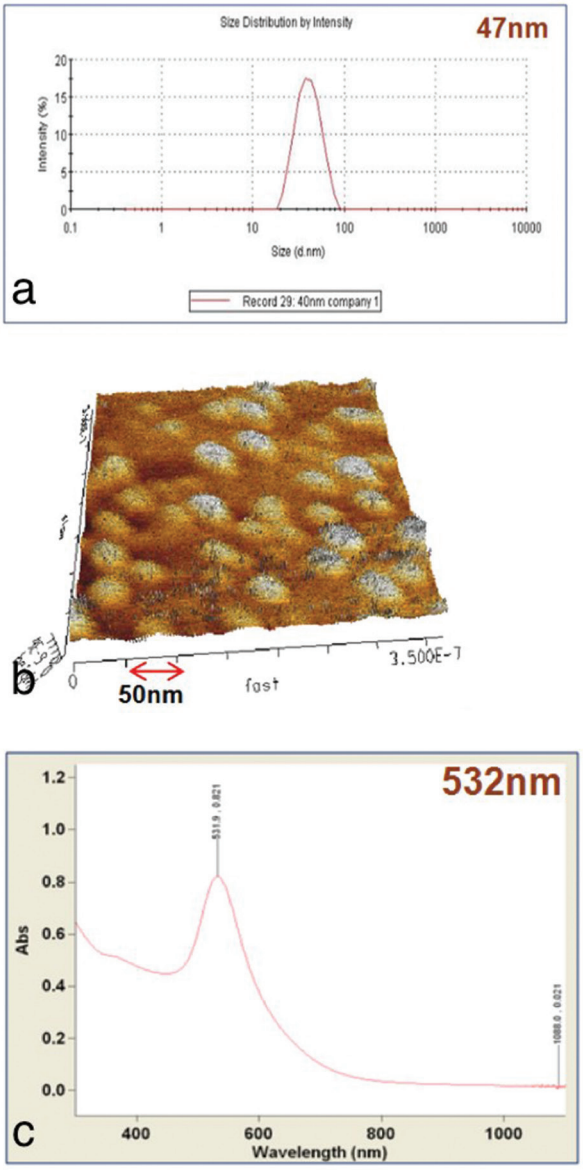

Figure 1. (a) DLS (b) AFM and (c) *UV/Vis* spectrophotometeric images showing the average size (47mm), shape (round), and absorption wavelength (532nm) of GNPs.

catheter with the same procedures as orthotopic bladder cancer model. A total of 0.4 ml conjugated anti-EGFR/GNP fragments were injected into the urinary bladder and held there for 30 min before irrigating the bladder twice using normal saline to wash out the unbound GNPs. A 2 cm incision was made in the lower abdomen of the mice to enable exploration of the urinary bladder. The bladder was separated from the surrounding organs using a piece of clean, wet gauze. A green laser (532nm) was then applied to the urinary bladder at a power setting of 10W/cm^2 and a frequency of 1.6Hz for 500 shots of 300ms each. During this procedure, normal saline in wet gauze was applied to the urinary bladder at a rate of 6ml/min to prevent overheating and protect the surrounding organs. The control group underwent the same surgical and laser procedures without instillation of conjugated GNPs. The mice were sacrificed at 2 weeks following the implantation of cancer cells, at which point the urinary bladder was resected for pathological review.

4. RESULTS

4.1. Preparation and characterization of GNPs

The average size and shape of the gold nanoparticles was characterized using dynamic light scattering (DLS) and atomic force microscopy (AFM). The particles appeared spherical in shape with an average diameter of 47 nm. UV/Vis spectrophotometry revealed that the absorption spectrum was approximately 532 nm. The wavelength of the laser system used in this study overlapped the absorption region of the GNPs, thereby ensuring the thermal efficiency of the system (Figure 1).

4.2. Overexpression of EGFR in cancer cell lines

Anti-EGFR antibodies were also used to quantify the expression of receptors in TCC cells. The antigens were found to be overexpressed on the membrane of urothelial bladder cancer cells, as confirmed using flow cytometry and confocal microscopy (Figure 2 and Figure 3). These observations demonstrate the pronounced expression of EGFR on tumor cells.

4.3. Interaction between GNPs and antibody fragments

Protein electrophoresis was used to confirm the molecular weight of anti-EGFR antibody fragments. Figure 4 illustrates the reduction of disulphide bonds and changes in molecular weight under a variety of conditions. The molecular weight of the antibody fragments was half that of the original antibodies (IgG). Reactions between GNPs and antibody fragments were evaluated (Figure 5) in order to determine a suitable bonding ratio. The molecular weight of antibody fragments influences their dispersion; therefore, we substituted the fragments for the original IgG in order to improve the dispersion of nanogold colloids. As GNPs present excellent affinity to sulfhydryl groups, the exposed disulphide bonds on the antibody fragments improve the process of combination and ultimate stability of the resulting molecules.

4.4. SEM and TEM images

Scanning electron microscopy (SEM) and transmission electron microscopy (TEM) were used to confirm the presence of anti-EGFR/GNP fragments and to observe the distribution of gold. SEM images of MBT2 cells are presented in Figure 6, in which anti-EGFR/GNP fragments are clearly bound to the MBT2 in various regions of the cells. As shown in the EDS

© 1996-2016

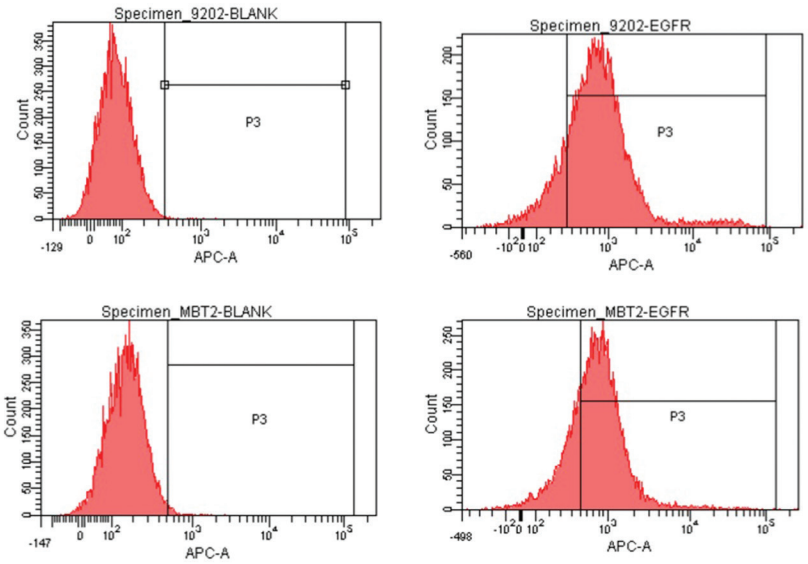

Figure 2. Results of flow cytometry reveal the strong expression of EGFR in MBT2 and 9202 cell lines.

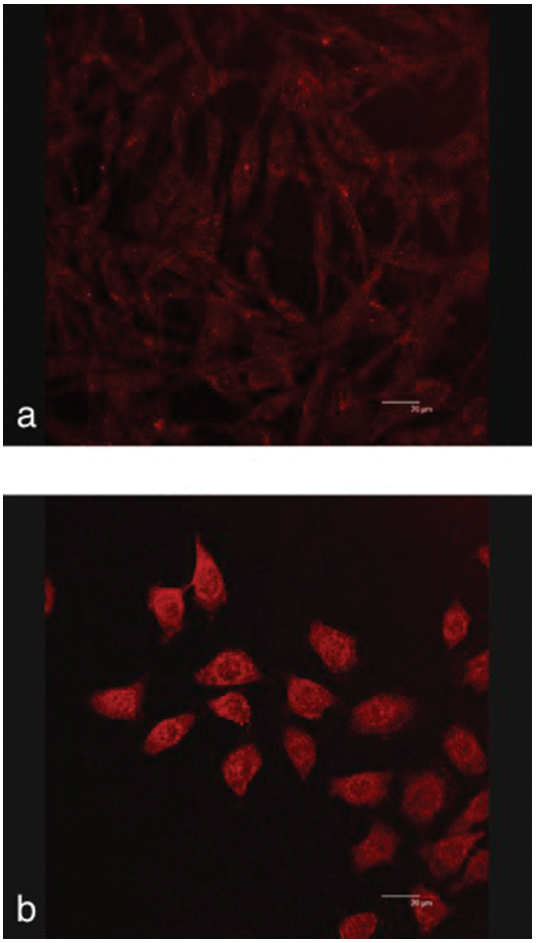

Figure 3. Confocal microscopic image showing EGFR expression in (a) MBT2 and (b) 9202 cell lines.

analysis (Figure 6), the weight of the gold accounted for 5.36 % of the total element content, thereby confirming the existence of GNPs. Figure 7 presents TEM images of MBT2 cell lines, clearly differentiating between cells with and without anti-EGFR/GNP fragments.

4.5. Photo thermal therapy of TCC cells

Various types of TCC cells(MBT2, and 9202) were used to test the efficacy of the photo thermal treatment. Figure 8 reveals that the cancer cells treated with GNPs were damaged at energy levels (500 shots, 300 ms in duration, power and frequency of 10 W/cm^2 and 1.6Hz, respectively) 3x lower than those required to damage cells that did not undergo GNP treatment. In addition, the use of GNPs with antibody fragments facilitated tumor targeting and improved treatment efficiency. This method may help facilitate the development of individualized therapies which employ different antigens to target specific types of cancer cells.

4.6. Measurement of variations in temperature

Temperatures were monitored throughout the testing period to facilitate comparison between treatment and control groups. Figure 9 reveals that the group which received anti-EGFR/GNPs treatment (i.e. the MBT2 cell line) was associated with an increase in temperature of 26.3 ºC to 43.2~45 ºC. In contrast, the control group presented an increase in temperature to only 34.4 ºC. Note that the temperature in the cancer cells beneath the surface in the vicinity of the GNPs should be higher than the reported temperatures because measurements were obtained in the medium surrounding the treatment area. Protein degeneration occurred when the temperature exceeded 40 ºC. In the

© 1996-2016

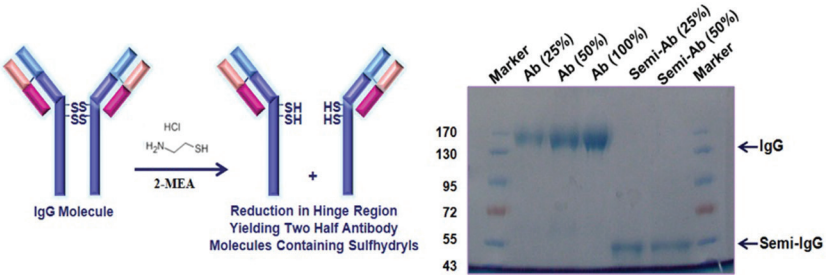

Figure 4. (left) Diagram illustrating the reduction reaction and (right) results from electrophoresis confirming that IgG was reduced

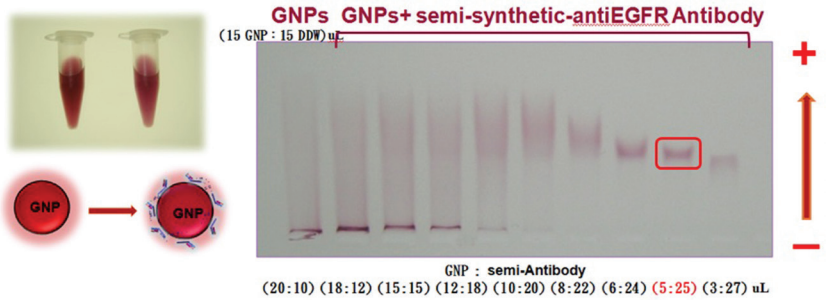

Figure 5. Tests used in the prepartion of antibody fragments for conjugation with GNPs. A ratio of 5:25 appeared to yield optimal conjugation results.

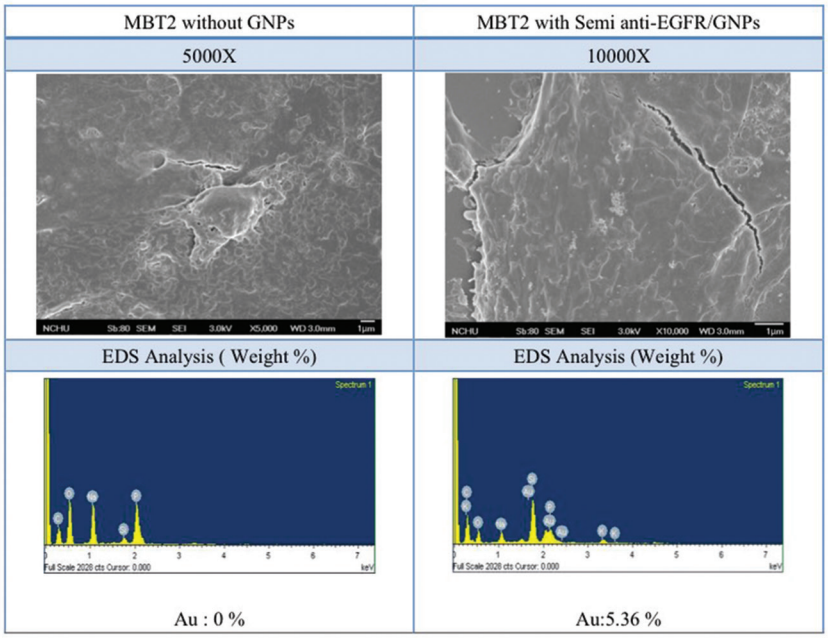

Figure 6. SEM and EDS analyses showing the binding of MBT2 cells to anti-EGFR antibody fragments conjugated with GNPs.

treatment group, exposure to 500 laser shots led to an increase in temperature that was sufficient to initiate the death of tumor cells due to a change in molecular configuration, the destruction of bonds, and alterations to the cell membrane.

4.7. Photothermal therapy: *in vivo*

Three days post-implantation of BMT2 cells in mice, five of the animals underwent laser treatment with conjugated anti-EGFR/GNP and five of the animals underwent sham procedures (control). At 2 weeks

© 1996-2016

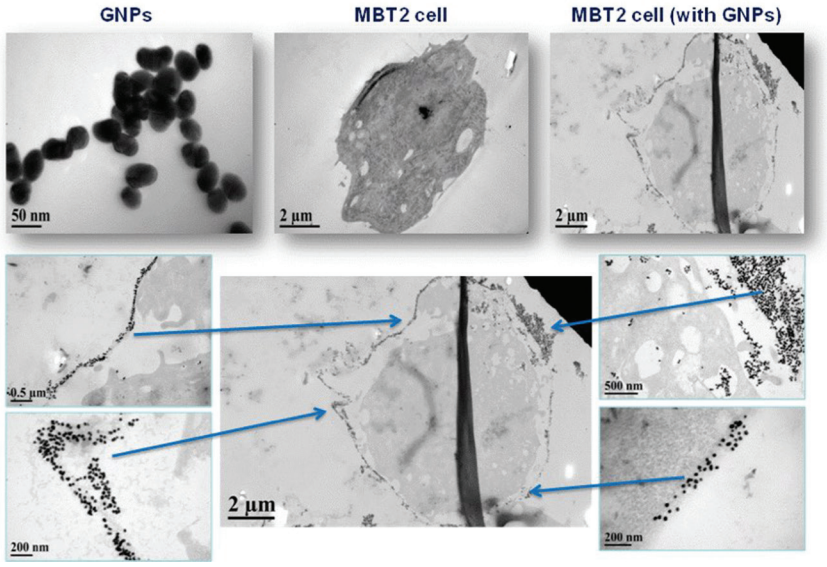

Figure 7. TEM images showing MBT2 cell lines (with and without GNP treatment). The GNPs with anti-EGFR antibody fragments bonded to the membrane of the cancer cells, resulting in endocytosis.

	10W/cm^2 without GNPs	10W/cm^2 with semi anti-EGFR antibody/ GNPs
MBT2	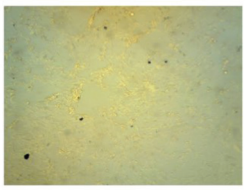	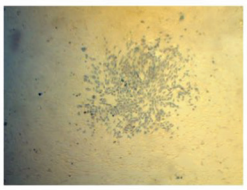
9202		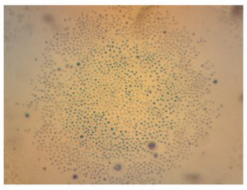

Figure 8. The energy required to kill cancer cells was far less than that required to kill normal cells.

post-implantation, 1 out of 5 treated mice (20%) displayed signs of tumor growth, while 4 out of 5 control group animals (80%) presented tumor growth ($p<0.0.5$). We also observed the development of a typical transparent TCC on the mucosal layer and transitional cells were overgrown (exceeding six layers). Cell nuclei presented a variety of diameters and distributions, including multiple nuclei in a single cell. Sections of the bladder obtained from treated mice are presented in Figure 10(a). The left side of the picture presents a normal urothelial epithelium with no distinct histological changes, which shows that treatment had minimal influence on normal cells. In contrast, the abnormal cells on the right side of picture reveal the presence of extensive coagulative necrosis, with large quantities of necrotic tissue accumulated on the mucosa. This is assumed to be the site of tumor implantation. Marked lymphocytes infiltration was noticed in the epithelium. Furthermore, the tissue structure in the abnormal area appears to have been loosened as a result of the treatment and even shows signs that the surface layer may be ready to fall off. Figure 10(b) shows that the tumor site was extensively damaged by necrosis (i.e. there are no discernible tumor cells); however, it is also clear that the overall architecture of subepithelial stroma and muscularis propria was maintained. Changes in the cell nucleus were the major morphological indication of cell necrosis. Specifically, contractions, fragmentation, and dissolution of the nuclei demonstrate the disintegration of cancer cells. These are clear indications that PTT had a stronger influence on tumor cells than it did on normal tissue, as shown in Figure 10(c).

5. DISCUSSION

The excellent photothermal properties of GNPs have led to their application in a variety of treatment techniques which target cancer cells (22, 30, 31). For example, GNPs can be used to rapidly detect abnormal genes or cancer cells, which improves cancer diagnosis and treatment. In addition, GNPs possess good biocompatibility, good modulability, non-cytoxicity, and highly specific optical properties. These characteristics suggest that GNPs can benefit a far wider range of clinical applications.

PTT has proven highly effective in the treatment of many types of tumors, including the *in vitro* treatment

© 1996-2016

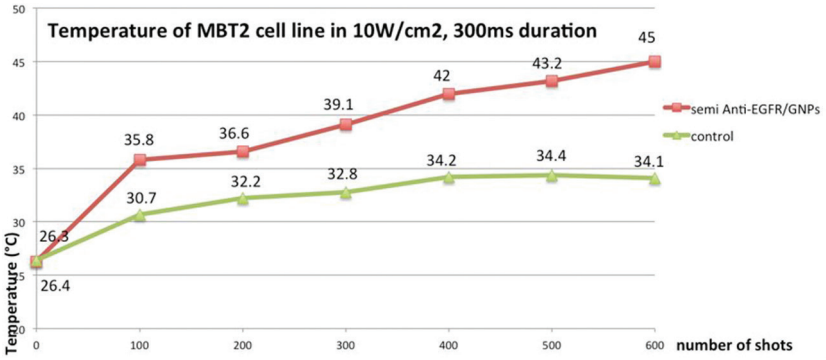

Figure 9. Increase in temperature during laser treatment of control cells (26.4.°C to 34.4.°C) and during laser treatment of MBT2 cells treated with GNPs and anti-EGFR antibody fragments (from 26.3.°C to 43°C ~45°C).

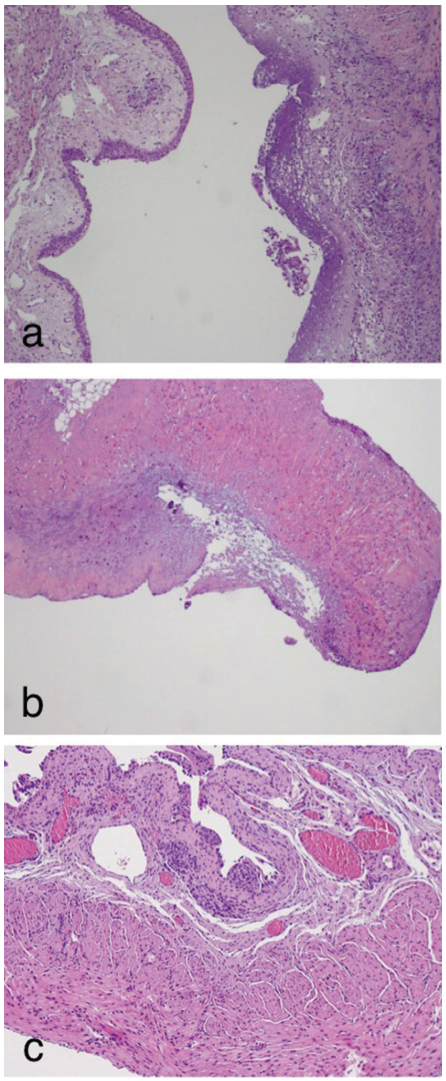

Figure 10. (a) The left side of the mucosa was unaffected by PTT, whereas the right side shows the tumor (implantation area), extended necrosis, and loosening of mucosa layer; (b) there is extensive necrosis in area where the tumor was destroyed; however, the structure of submucosa and the muscle layers were preserved; (c) control group mucosa and submucosa layers showing tumor growth.

of urothelial cancers (22). This study performed *in vivo* treatment using an orthotopic bladder cancer model in mice. Our encouraging results indicate that further animal studies using larger animals with bladders that more closely mimic those of humans are warranted.

Antibody itself can be conjugated with GNPs due to differences in the electrical charges between GNPs and proteins (10, 21, 22). However, this form of conjugation lacks uniformity because the functional part of the antibody fragments is not always lined up. In addition, following the conjugation of antibody fragments, the GNPs become heavier and therefore even more likely to precipitate, potentially within a short few hours. To overcome this problem, we first reduced antibody fragments to achieve stable conjugation with GNPs. We chose this strategy based on the fact that the affinity of disulphide bonds to GNPs is far stronger than the affinity of different charges between the antibody and GNPs. In addition, the antibody fragments are well-oriented, such that the functional part always faces outward. In this study, a reduction in the weight of the assembled nanoparticles and the uniformity of the antibody fragments on the GNPs prevented the precipitation of the solution; however, a long-term study on the stability of the particles is required to confirm our findings.

This study focused on superficial bladder cancers, due to the fact that these types of cancer have a very high recurrence rate (up to 70%) in the first 5 years following TURBT. If the tumor is resected prior to muscle invasion, the bladder can be preserved. However, if resection is delayed, then the resulting urinary diversion can have a tremendous impact on quality of life. Adjuvant intravesical therapies after TURBT have proven highly successfully in delaying recurrence; however, they have no effect on the overall recurrence rate or long-term survival. PTT is able to target cancer cells directly by inducing antigen-antibody reactions and destroying cancer cells by the heat generated in PTT. This pilot study demonstrates the potential for killing cancer cells in the very early stages and thereby preventing tumor growth and seeding. Adoption of this method would not require

© 1996-2016

that urologists alter their routine practices, due to the fact that the conjugated GNPs are introduced into the urinary bladder using a catheter and the laser is applied under cystoscopy assistance. The GNPs are then washed out by the urine, such that the theoretical likelihood of deposition in vital organs, such as the brain, lung, or liver, is very low. However, additional animal experiments are required to confirm this supposition.

Numerous tumor markers and specific antigens, such as EGFR and Mucin 7, in urothelial cancer have been studied. The method we used to reduce antibody fragments could be applied to a variety of markers according to characteristics of the specific cancer cells, thereby facilitating the development of individualized therapy.

6. CONCLUSION

The use of PTT and GNPs conjugated with antibody fragments allows specific cancer cells to be targeted by low energy lasers, which avoids damage to normal tissue. This approach enables the early targeting of tumors so that the tumors can be killed before they were visible. Besides, the assembled GNPs will be voided out soon after the treatment so that there is less opportunity for the GNPs to deposit in the body. Thus, our method represents a highly promising adjuvant treatment choice for superficial bladder cancer. However, despite the promising results in a mouse orthotopic bladder cancer model, additional studies which employ larger animals are required to confirm the efficacy of our method and to further develop the design of laser probes.

7. ACKNOWLEDGEMENT

Authors declare no conflict of interest.

8. REFERENCES

1. D. L. Lamm and F. M. Torti: Bladder cancer, 1996. *CA Cancer J Clin*, 46(2), 93-112 (1996) DOI: 10.3322/canjclin.46.2.93
2. A. Quintero, J. Alvarez-Kindelan, R. J. Luque, R. Gonzalez-Campora, M. J. Requena, R. Montironi and A. Lopez-Beltran: Ki-67 MIB1 labelling index and the prognosis of primary TaT1 urothelial cell carcinoma of the bladder. *J Clin Pathol*, 59(1), 83-8 (2006) DOI: 10.1136/jcp.2004.022939
3. M. Puntoni, S. Zanardi, D. Branchi, S. Bruno, A. Curotto, M. Varaldo, P. Bruzzi and A. Decensi: Prognostic effect of DNA aneuploidy from bladder washings in superficial bladder cancer. *Cancer Epidemiol Biomarkers Prev*, 16(5), 979-83 (2007) DOI: 10.1158/1055-9965.EPI-06-0538
4. Z. Kirkali, T. Chan, M. Manoharan, F. Algaba, C. Busch, L. Cheng, L. Kiemeney, M. Kriegmair, R. Montironi, W. M. Murphy, I. A. Sesterhenn, M. Tachibana and J. Weider: Bladder cancer: epidemiology, staging and grading, and diagnosis. *Urology*, 66(6 Suppl 1), 4-34 (2005) DOI: 10.1016/j.urology.2005.07.062
5. R. J. Sylvester, M. A. Brausi, W. J. Kirkels, W. Hoeltl, F. Calais Da Silva, P. H. Powell, S. Prescott, Z. Kirkali, C. van de Beek, T. Gorlia and T. M. de Reijke: Long-Term Efficacy Results of EORTC Genito-Urinary Group Randomized Phase 3 Study 30911 Comparing Intravesical Instillations of Epirubicin, Bacillus Calmette-Guerin, and Bacillus Calmette-Guerin plus Isoniazid in Patients with Intermediate- and High-Risk Stage Ta T1 Urothelial Carcinoma of the Bladder. *Eur Urol,* 57, 766-773 (2010) DOI: 10.1016/j.eururo.2009.12.024
6. M. D. Shelley, H. Kynaston, J. Court, T. J. Wilt, B. Coles, K. Burgon and M. D. Mason: A systematic review of intravesical bacillus Calmette-Guerin plus transurethral resection vs transurethral resection alone in Ta and T1 bladder cancer. *BJU Int*, 88(3), 209-16 (2001) DOI: 10.1046/j.1464-410x.2001.02306.x
7. T. Gardmark, S. Jahnson, R. Wahlquist, H. Wijkstrom and P. U. Malmstrom: Analysis of progression and survival after 10 years of a randomized prospective study comparing mitomycin-C and bacillus Calmette-Guerin in patients with high-risk bladder cancer. *BJU Int*, 99(4), 817-20 (2007) DOI: 10.1111/j.1464-410X.2006.06706.x
8. L. Au, D. Zheng, F. Zhou, Z. Y. Li, X. Li and Y. Xia: A quantitative study on the photothermal effect of immuno gold nanocages targeted to breast cancer cells. *ACS Nano*, 2(8), 1645-52 (2008) DOI: 10.1021/nn800370j
9. M. Eghtedari, A. V. Liopo, J. A. Copland, A. A. Oraevsky and M. Motamedi: Engineering of hetero-functional gold nanorods for the *in vivo* molecular targeting of breast cancer cells. *Nano Lett*, 9(1), 287-91 (2009) DOI: 10.1021/nl802915q
10. I. H. El-Sayed, X. Huang and M. A. El-Sayed: Selective laser photo-thermal therapy of epithelial carcinoma using anti-EGFR antibody conjugated gold nanoparticles. *Cancer Lett*,

© 1996-2016

239(1), 129-35 (2006)
DOI: 10.1016/j.canlet.2005.07.035

11. X. H. Huang, I. H. El-Sayed, W. Qian and M. A. El-Sayed: Cancer cell imaging and photothermal therapy in the near-infrared region by using gold nanorods. *Journal of the American Chemical Society*, 128(6), 2115-2120 (2006)
DOI: 10.1021/ja057254a

12. F. Y. Cheng, C. T. Chen and C. S. Yeh: Comparative efficiencies of photothermal destruction of malignant cells using antibody-coated silica@Au nanoshells, hollow Au/Ag nanospheres and Au nanorods. *Nanotechnology*, 20(42), 425104 (2009)
DOI: 10.1088/0957-4484/20/42/425104

13. G. R. Reddy, M. S. Bhojani, P. McConville, J. Moody, B. A. Moffat, D. E. Hall, G. Kim, Y. E. Koo, M. J. Woolliscroft, J. V. Sugai, T. D. Johnson, M. A. Philbert, R. Kopelman, A. Rehemtulla and B. D. Ross: Vascular targeted nanoparticles for imaging and treatment of brain tumors. *Clin Cancer Res*, 12(22), 6677-86 (2006)
DOI: 10.1158/1078-0432.CCR-06-0946

14. W. Lin, Y. W. Huang, X. D. Zhou and Y. Ma: Toxicity of cerium oxide nanoparticles in human lung cancer cells. *Int J Toxicol*, 25(6), 451-7 (2006)
DOI: 10.1080/10915810600959543

15. I. S. Kim, M. Baek and S. J. Choi: Comparative cytotoxicity of Al2O3, CeO2, TiO2 and ZnO nanoparticles to human lung cells. *J Nanosci Nanotechnol*, 10(5), 3453-8 (2010)
DOI: 10.1166/jnn.2010.2340

16. C. Hanley, J. Layne, A. Punnoose, K. M. Reddy, I. Coombs, A. Coombs, K. Feris and D. Wingett: Preferential killing of cancer cells and activated human T cells using ZnO nanoparticles. *Nanotechnology*, 19(29), 295103 (2008)
DOI: 10.1088/0957-4484/19/29/295103

17. Y. M. Huh, Y. W. Jun, H. T. Song, S. Kim, J. S. Choi, J. H. Lee, S. Yoon, K. S. Kim, J. S. Shin, J. S. Suh and J. Cheon: *In vivo* magnetic resonance detection of cancer by using multifunctional magnetic nanocrystals. *J Am Chem Soc*, 127(35), 12387-91 (2005)
DOI: 10.1021/ja052337c

18. X. Gao, Y. Cui, R. M. Levenson, L. W. Chung and S. Nie: *In vivo* cancer targeting and imaging with semiconductor quantum dots. *Nat Biotechnol*, 22(8), 969-76 (2004)
DOI: 10.1038/nbt994

19. Q. Liu, Y. Q. Ge, F. Q. Li, S. X. Zhang, N. Gu, Z. Q. Wang and G. M. Lu: (Biological activity assays and cellular imaging of anti-human sperm protein 17 immunomagnetic nanoparticles). *Xi Bao Yu Fen Zi Mian Yi Xue Za Zhi*, 25(11), 987-90 (2009)
DOI: 10.1016/j.canlet.2008.09.024

20. H. J. Huisman, J. J. Futterer, E. N. van Lin, A. Welmers, T. W. Scheenen, J. A. van Dalen, A. G. Visser, J. A. Witjes and J. O. Barentsz: Prostate cancer: precision of integrating functional MR imaging with radiation therapy treatment by using fiducial gold markers. *Radiology*, 236(1), 311-7 (2005)
DOI: 10.1148/radiol.2361040560

21. C. J. Ackerson, M. T. Sykes and R. D. Kornberg: Defined DNA/nanoparticle conjugates. *Proc Natl Acad Sci U S A*, 102(38), 13383-5 (2005)
DOI: 10.1073/pnas.0506290102

22. C. H. Chen, Y. J. Wu and J. J. Chen: Gold nanotheranostics: photothermal therapy and imaging of mucin 7 conjugated antibody nanoparticles for urothelial cancer. *Biomed Res Int*, 2015, 813632 (2015)
DOI: 10.1155/2015/813632

23. G. J. Villares, M. Zigler, K. Blehm, C. Bogdan, D. McConkey, D. Colin and M. Bar-Eli: Targeting EGFR in bladder cancer. *World J Urol*, 25(6), 573-9 (2007)
DOI: 10.1007/s00345-007-0202-7

24. M. Kinjo, T. Okegawa, S. Horie, K. Nutahara and E. Higashihara: Detection of circulating MUC7-positive cells by reverse transcription-polymerase chain reaction in bladder cancer patients. *Int J Urol*, 11(1), 38-43 (2004)
DOI: 10.1111/j.1442-2042.2004.00739.x

25. A. Bhatia, P. Dey, Y. Kumar, U. Gautam, N. Kakkar, R. Srinivasan and R. Nijhawan: Expression of cytokeratin 20 in urine cytology smears: a potential marker for the detection of urothelial carcinoma. *Cytopathology*, 18(2), 84-6 (2007)
DOI: 10.1111/j.1365-2303.2006.00432.x

26. J. Kimling, M. Maier, B. Okenve, V. Kotaidis, H. Ballot and A. Plech: Turkevich method for gold nanoparticle synthesis revisited.

© 1996-2016

Journal of Physical Chemistry B, 110(32), 15700-15707 (2006)
DOI: 10.1021/jp061667w

27. J. D. Hirsch and R. P. Haugland: *Methods in Molecular Biology, vol. 295: Immunochemical Protocols Third Edition,* 135-154 (2005)
DOI: 10.1385/1-592**2**59-873-0:135

28. S. Yoshitake, Y. Yamada, E. Ishikawa and R. Masseyeff: Conjugation of glucose oxidase from Aspergillus niger and rabbit antibodies using N-hydroxysuccinimide ester of N-(4-carboxycyclohexylmethyl)-maleimide. *Eur J Biochem*, 101(2), 395-9 (1979)
DOI: 10.1111/j.1432-1033.1979.tb19731.x

29. Z. Xiao, T. J. McCallum, K. M. Brown, G. G. Miller, S. B. Halls, I. Parney and R. B. Moore: Characterization of a novel transplantable orthotopic rat bladder transitional cell tumour model. *Br J Cancer*, 81(4), 638-46 (1999)
DOI: 10.1038/sj.bjc.6690741

30. W. Lu, S. R. Arumugam, D. Senapati, A. K. Singh, T. Arbneshi, S. A. Khan, H. Yu and P. C. Ray: Multifunctional oval-shaped gold-nanoparticle-based selective detection of breast cancer cells using simple colorimetric and highly sensitive two-photon scattering assay. *ACS Nano*, 4(3), 1739-49 (2010)
DOI: 10.1021/nn901742q

31. G. von Maltzahn, J. H. Park, A. Agrawal, N. K. Bandaru, S. K. Das, M. J. Sailor and S. N. Bhatia: Computationally guided photothermal tumor therapy using long-circulating gold nanorod antennas. *Cancer Res*, 69(9), 3892-900 (2009)
DOI: 10.1158/0008-5472.CAN-08-4242

Key Words: Photothermal Therapy, Gold Nanoparticles, Urothelial Cancer, Target Therapy

Send correspondence to: Chieh Hsiao Chen, 123 Sin-der Rd., Beigang, Yunlin, Taiwan, Tel: 886922308059, Fax: 886423127868, E-mail: jerrychen119@gmail.com

© 1996-2016